STABILITY ANALYSIS OF INTENSE ION BEAMS IN THE NIRS S-RING

V. Kapin, M. Kanazawa, T. Murakami, K. Noda, S. Yamada, NIRS, Chiba;
E. Syresin, JINR, Dubna, Moscow Region;
S. Shibuya, Sumitomo Heavy Industries, Tokyo

Abstract

A small ring (S-ring) with circumference of 25 m has been proposed at NIRS. It will produce an ion beam with intensity higher $5\cdot10^9$ particle per second (pps), the injection energy of 6 MeV/u, the output energy of 1-28 MeV/u for charge to mass ratio of 0.5 and bunch length of 10-1000 ns. The main peculiarities of S-ring are the low energy after deceleration and the small circumference. A feature of S-ring is a large relative length of the cooling section, which occupies 3.6 % of the ring circumference. This value is 3-5 times higher than in the usual ion storage rings. A maximum intensity of cooled ion beam can be restricted by the ion beam instabilities. The application of intense electron beam for fast cooling of ion beam in the S-ring is limited so-called effect of electron heating. The stability analysis includes the following effects: tune shift, longitudinal and transverse beam instabilities, space charge effects in the electron cooling system, multi-stream transverse instabilities. Results of analytical estimations and stability analysis are presented.

1 INTRODUCTION

A small synchrotron ring (S-ring) with circumference of 25 m has been proposed at NIRS [1,2]. The S-ring will provide heavy ion beams from proton to Xe for experimental users and to work as a booster ring for the HIMAC synchrotron in the future.

An outline of the lattice design had been described in Ref. [3]. S-ring will produce an ion beam with intensity higher $5\cdot10^9$ pps (the operation circle 1 Hz), from the injection energy of 6 MeV/u to the output energy of 1-28 MeV/u for charge to mass ratio of Z/A=0.5 and bunch length of 10-1000 ns. The electron cooler (EC) will be installed to realize a beam with a high intensity and small emittance. A multi-turn injection and cooling-stacking scheme [4] will be applied.

The stability analysis should include the following effects [5,6]: tune shift, longitudinal and transverse beam instabilities, space charge effects in the electron cooling system, multi-stream transverse instabilities. In this paper, some results of such analysis are presented.

2 STABILITY ANALYSIS

The electron cooling reduces a phase space V_{ps} occupied by an ion beam. If as result of the cooling, the density N/V_{ps} becomes larger than a given threshold, the ion beam becomes unstable [5]. For standard heavy ion machine this happens when the number of circulating particles exceeds $N=10^9$ [5]. Let's consider threshold values of N for wide ranges of transverse beam sizes and momentum spreads. The analysis will be done for coasting beam in the vertical plane.

2.1 Tune shift

For a uniform coasting beam of elliptical cross section with horizontal and vertical radii, a_x and a_y, tune shift due to the ion-beam space charge is given by [5-7]:

$$\Delta Q_y \approx \frac{r_p}{\pi}\cdot\frac{Z^2}{A}\cdot\frac{N(R/Q_y)F_{sc}}{\beta^2\gamma^3 a_y(a_x+a_y)}, \qquad (1)$$

where $r_p = 1.54\cdot10^{-18}$ m is the classical proton radius, A and Z are mass number and charge state number of ion (A=40 Z=18 for argon*), R is the ring mean radius (R=3.77 m), Q_y is the vertical bare tune (Q_y=1.35), F_{sc} is image-force correction factors ($F_{sc}\approx1$). The ratio of the beam radii is constant ($a_x/a_y=2$). The depressed tune Q_β^{d} is given by $Q_\beta^{\mathrm{d}}=\sqrt{Q_y^2+2Q_y\Delta Q_y}$ [7].

Figure 1 shows values of the depressed tune on the plane "a_y - N" at the injection energy W_{inj}=6 MeV/u (β=0.113 and γ=1.006). The number of circulating particles up to $N=10^{10}$ can be obtained at $a_y > 7$ mm with moderate values of tune shift $\Delta Q_y \le 0.1$.

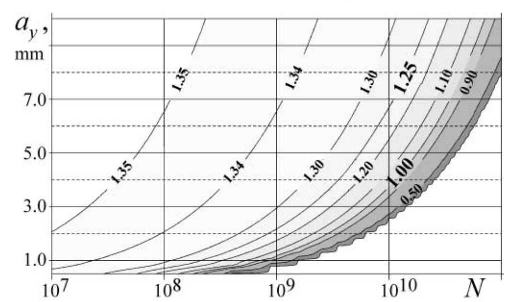

Figure 1: Values of Q_β^{d} on the plane "a_y - N".

2.2 Dispersion equation for dipole oscillations

The transverse coherent instabilities of unbunched beam and effects of Landau dumping have been described in Ref. [8-14]. The transverse dipole oscillations of the beam are given as $\langle y(s,t)\rangle \propto \exp[(-i\Omega t + in(s/R)]$, where s is the longitudinal coordinate, and n is the mode number. The coherent frequency, Ω is determined by the dispersion relation [9]:

* Constant values used for our calculations are given in brackets.

$$U_\perp + iV = \frac{g(u) + if(u)}{[f^2(u) + g^2(u)]S}, \qquad (2)$$

with $u = (\omega_\beta - \Omega - n\omega_0)S/\Delta\omega_\beta^{\mathrm{HWHM}}$, where ω_0 and ω_β are the angular frequencies of beam revolution and betatron oscillations, and $\Delta\omega_\beta^{\mathrm{HWHM}}$ is the HWHM betatron frequency spread given by:

$$\Delta\omega_\beta^{\mathrm{HWHM}} = \left|\xi + (n - Q_\beta^{\mathrm{d}})\eta\right|\overline{\omega}_0(\Delta\delta)_{\mathrm{HWHM}}, \qquad (3)$$

where $\Delta\delta_{\mathrm{HWHM}}$ is the beam momentum spread, ξ is the chromaticity (ξ=-5.1), $\eta = \gamma_{\mathrm{tr}}^{-2} - \gamma^{-2}$ is the slip factor (γ_{tr}=3.07). The beam response functions $g(u)$ and $f(u)$ and coefficient S are determined by the frequency spectrum of particle momentum distributions $\rho(\delta)$. The l.h.s. of the dispersion relation is expressed as

$$U_\perp + iV_\perp = -\frac{qcI_{\mathrm{b}}}{4\pi Q_\beta^{\mathrm{d}} E \Delta\omega_\beta^{\mathrm{HWHM}}} Z_1^\perp(n\omega_0 + \omega_\beta), \qquad (4)$$

where I_{b} is the beam current, q and E are the particle charge and energy, c is the velocity of light, and $Z_1^\perp(n\omega_0 + \omega_\beta)$ is the transverse coupling impedance.

The instability is generated by $\Omega \to \Omega + i\varepsilon$ with the growth rate, ε real and positive. This translates to $u \to u - i\varepsilon_u$, with the relation $\varepsilon_u = \varepsilon S/\Delta\omega_\beta^{\mathrm{HWHM}}$.

2.3 Transverse coupling impedances

The impedance $Z_1^\perp(n\omega_0 + \omega_\beta)$ is contributed by terms due to the space charge, $Z_{\mathrm{SC}}^\perp = (iZ_0R/\beta^2\gamma^2)(a_{\mathrm{eq}}^{-2} - b_{\mathrm{eq}}^{-2})$, resistive wall, $Z_{\mathrm{RW}}^\perp = -(1+i)Z_0R\delta_{\mathrm{skin}}/b_{\mathrm{eq}}^3$, and kicker, $Z_{\mathrm{K}}^\perp = -(Z_0l_{\mathrm{K}})/(2\pi h_{\mathrm{K}}^2)$ [5,6,8,9,12], where $Z_0 = 377\Omega$, a_{eq} is the equivalent beam radius given by $a_{\mathrm{eq}} = \sqrt{a_y(a_x + a_y)/2}$ [12], b_{eq} is the equivalent half-height of the elliptic vacuum chamber [15] ($b_{\mathrm{eq}} \approx 0.03$ m), δ_{skin} is the skin-depth at frequency ω given by $\delta_{\mathrm{skin}} = \sqrt{2/\omega\mu_0\sigma}$ ($\mu_0 = 4\pi \cdot 10^{-7}$ H/m, $\sigma = 1.4 \cdot 10^6$ $(\Omega \cdot \mathrm{m})^{-1}$), l_{K} and h_{K} are kicker length and half-height (l_{K}=0.4m, h_{K}=0.03m).

2.4 Stability diagram for the elliptic distribution

Let's approximate the momentum spectrum by the elliptic distribution, which looks to be a good approximation for the beam injected from the ion linac. The distribution function is given by [8,9]:

$$\rho(\upsilon) = \left(2S/\pi\Delta\omega^{\mathrm{HWHM}}\right)\sqrt{1-\upsilon^2}\,H\left(1 - |\upsilon|\right), \qquad (5)$$

where H is the Heaviside step function, and $S = \sqrt{3}/2$. The beam response functions are given by expressions $f(u) = 2[u - \mathrm{sgn}(u)]\sqrt{\upsilon^2 - 1}\,H(|\upsilon| - 1)$ with the sign-function, $\mathrm{sgn}(u)$, and $g(u) = 2\sqrt{1-\upsilon^2}\,H(1 - |\upsilon|)$. To interpret the dispersion relation, one should trace the locus of the r.h.s. of Eq. (2) on the complex plane as u is scanned from $-\infty$ to $+\infty$. The curves $\varepsilon_u = \mathrm{const}$ yield lines of equal growth rate. In particular, the curve $\varepsilon_u = 0$ is the "stability threshold". The l.h.s. of Eq. (2) yields a point $U_\perp + iV_\perp$ on the same complex plane. Figure 2 shows three curves of $\varepsilon_u = 0$, $\varepsilon_u = 0.1$ and $\varepsilon_u = 0.2$ for the elliptical distribution. If the point $U_\perp + iV_\perp$ is surrounded by the curve $\varepsilon_u = 0$, the beam is stable. Otherwise the point $U_\perp + iV_\perp$ coincides with some curve of $\varepsilon_u = \mathrm{const}$ and the beam is unstable.

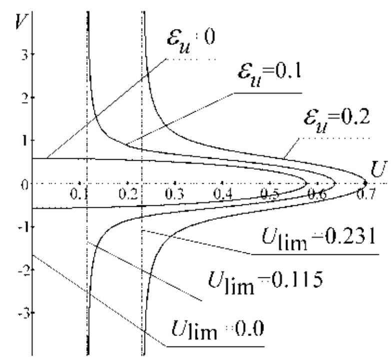

Figure 2:Stability diagram for the elliptic distribution.

For the elliptical distribution the threshold curve on the "$U - V$"-plane is a semi-circle of radius $1/\sqrt{3}$. It coincides with the Keil-Schnell type of stability circle [8,9,13] with the stability condition written as $|U_\perp + iV_\perp| \le 1/\sqrt{3}$. The widely used Schnell-Zotter criterion [14] with radius $2/\pi$ differs less than 10%.

At a high beam current $|U_\perp| << |V_\perp|$, and the r.h.s. of Eq. (2) can be approximated by the asymptote $U_{\mathrm{lim}} \approx 4\varepsilon_u S/3$. It provides the approximate expression for the growth rate

$$\varepsilon \approx qcI_{\mathrm{b}}\,\mathrm{Re}[Z_1^\perp(n\omega_0 + \omega_\beta)]/4\pi Q_\beta^{\mathrm{d}} E. \qquad (6)$$

This expression is the same as for beam with zero momentum spread (see for example Ref [10, p.210]).

2.5 The stability diagram for S-ring

The dispersion relation (2) has been solved numerically. Figure 3 shows the diagram for logarithmic values of instability growth rate, $\log\varepsilon$ at two values of momentum spread. The stable area with Landau dumping depends on $\Delta\delta_{\mathrm{HWHM}}$. In the S-ring, an acceleration circle lasts about 0.5 s, and permitted growth time is limited by this value. For $\Delta\delta_{\mathrm{HWHM}} \le 0.1\%$, $a_y < 10\mathrm{mm}$ and $N = 5 \cdot 10^9$, the instability growth-time is very short, $\tau = 1/\varepsilon \approx 0.1\,\mathrm{s}$ (the line $\log\varepsilon = 1.0$ in Fig.3). At $\Delta\delta_{\mathrm{HWHM}} \le 0.1\%$, only large beams with $a_y \ge 10\mathrm{mm}$ can be stabilized for $N \ge 2 \cdot 10^9$.

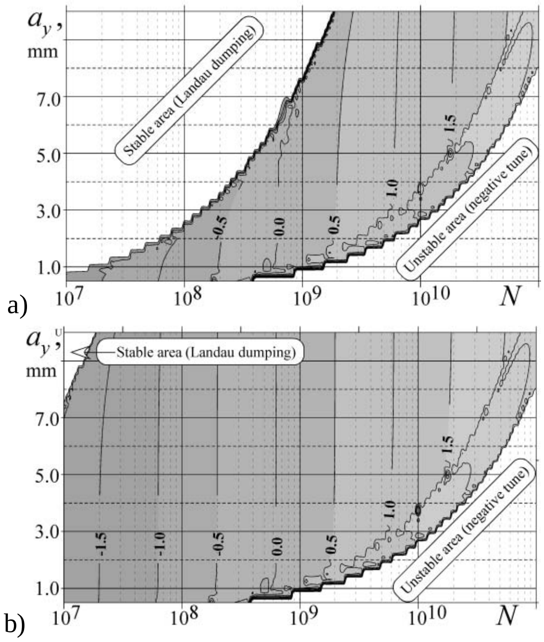

Figure 3: Diagram for logarithmic values of ε at $\Delta\delta_{\mathrm{HWHM}}$ =0.1 % (a) and $\Delta\delta_{\mathrm{HWHM}}$ =0.001 % (b).

A feature of S-ring is the low energy after deceleration. Figure 4 shows diagram for the beam energy W_{out} =1 MeV/u at $\Delta\delta_{\mathrm{HWHM}}$ =0.1 %. In comparison with diagrams for the injection energy, the unstable area with negative tunes and the stable area with Landau dumping are shifted to the low values of N . The instability growth rates are reduced.

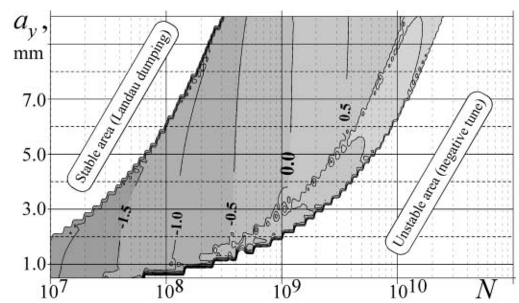

Figure 4: Diagram for logarithmic values of ε at $\Delta\delta_{\mathrm{HWHM}}$ =0.1 % and beam energy W_{out} =1 MeV/u.

2.6 The stability diagram with electron cooling

An electron beam of EC presents large impedance to the circulating ion beam. Coupling impedances of EC has been introduced in Ref. [16]. A real part of the EC-impedance responsible for instabilities is given by [6]:

$$Z_{\mathrm{EC}}^{\perp} \approx -5.5 Z_0 R \eta_{\mathrm{EC}} \sqrt{n_e r_e} \Big/ \beta^2 a_e \,, \qquad (7)$$

where $r_e = 2.82 \cdot 10^{-15}$ m is classical electron radius, a_e, $n_e = I_e / e\beta c \pi\, a_e^2$, I_e are electron beam radius (1cm), density, and current, respectively. The relative length of EC for S-ring, $\eta_{\mathrm{EC}} = l_{\mathrm{EC}} / 2\pi R$ =3.6% is 3-5 times higher than in usual storage rings. From Eqs. (6) and (7), one gets that the growth rate depends on electron current as $\varepsilon \propto I_e^{1/2}$. Figure 5 shows stability diagram calculated with EC-impedance (7) at I_e =0.1A. The growth-rates are 20-30 times higher in comparison with the "EC-off" case (see Fig.3,a). Note, that instabilities can be partially or completely suppressed at high cooling rates [16].

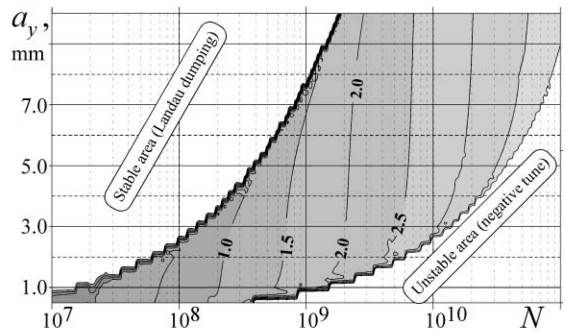

Figure 5: Diagram for logarithmic values of ε at $\Delta\delta_{\mathrm{HWHM}}$ =0.1 % and I_e =0.1A.

2.7 Other instabilities

S-ring will operate below transition. The imaginary part of longitudinal impedance due to the space charge, $\mathrm{Im}(Z_{\mathrm{SC}}^{\parallel})$ is about several tens of $\mathrm{k}\Omega$. In this case, there cannot be longitudinal instabilities. This is explained by the "thermometer shape" of stable area [6].

S-ring will provide ion beams with bunch length of 10-1000 ns using a bunch rotation technique [1,2]. Results of numerical simulations with space-charge effects had been reported in paper [17].

Multi-stream instabilities [5,6,9,18] due to interactions between circulating ion beam, secondary electrons, electron beam of EC, and secondary ions also can be generated in S-ring. Analysis of these instabilities is a subject of future studies.

3 REFERENCES

[1] K. Noda et al., report HIMAC-017, p.1-33 (1997).
[2] K. Noda et al., "S-ring Project at NIRS", these Proceedings, paper THPLE099.
[3] S. Shibuya et al, Proc. EPAC-98, pp. 547-549 (1998).
[4] T. Tanabe et al, N.I.M., A307, pp.7-25(1991).
[5] J. Bosser, CERN 95-06, Vol. 2, pp. 673-730.
[6] J. Bosser et al, N.I..M., A441, pp.1-8 (2000).
[7] K.Y. Ng, FERMILAB-TM-2152 (2001).
[8] A.W. Chao, "Physics of Collective Beam Instabilities in High Energy Accelerators", Wiley, N.Y., 1993.
[9] K.Y. Ng, US P.A.S., FERMILAB-FN-0713 (2002).
[10] A. Hofmann, CERN 95-06, pp. 275-331.
[11] B. Zotter, F. Sacherer, CERN 77-13, pp. 175-218.
[12] "Handbook of Accelerator Physics and Engineering", ed. A.W. Chao and M.Tigner, World Scientific, 1999.
[13] E. Keil, W. Schnell, CERN-ISR-TH-RF/69-48.
[14] W. Schnell, B. Zotter, CERN-ISR-GS-RF/76/26.
[15] L. Palumbo et al, CERN 95-06, pp. 331-390.
[16] A. Burov, Proc. PAC'95, pp.3055-3058.
[17] K. Ohtomo et al, Proc. EPAC-2000, pp. 1540-1542.
[18] A. Burov, CERN 94-03, p.230-234.